CHEMISTRY
AN ASIAN JOURNAL
ACES
FULL PAPER

DOI: 10.1002/asia.201200726

1-Aryl-4-Silylmethyl[60]fullerenes: Synthesis, Properties, and Photovoltaic Performance

Yutaka Matsuo,*[a] Hiromi Oyama,[a] Iwao Soga,[a, b] Toshihiro Okamoto,[a, d] Hideyuki Tanaka,[a] Akinori Saeki,[c] Shu Seki,[c] and Eiichi Nakamura*[a]

Abstract: The efficient nucleophilic addition of aryl Grignard reagents (aryl = 4-$MeOC_6H_4$, 4-$Me_2NC_6H_4$, Ph, 4-$CF_3C_6H_4$, and thienyl) to C_{60} in the presence of DMSO produced 1,2-arylhydro[60]fullerenes after acid treatment. The reactions of the anions of these arylhydro[60]fullerenes with either dimethylphenylsilylmethyl iodide or dimethyl(2-isopropoxyphenyl)silylmethyl iodide yielded the target compounds, 1-aryl-4-silylmethyl[60]fullerenes. The properties and structures of these 1-aryl-4-silylmethyl[60]fullerenes (aryl = 4-$MeOC_6H_4$, thienyl) were examined by electrochemical studies, X-ray crystallography, flash-photolysis time-resolved microwave-conductivity (FP-TRMC) measurements, and electron-mobility measurements by using a space-charge-limited current (SCLC) model. Organic photovoltaic devices with a polymer-based bulk heterojunction structure and small-molecule-based *p–n* and *p–i–n* heterojunction configurations were fabricated by using 1-aryl-4-silylmethyl[60]fullerenes as an electron acceptor. The most efficient device exhibited a power-conversion efficiency of 3.4 % (short-circuit current density: 8.1 mA/cm^2, open-circuit voltage: 0.69 V, fill factor: 0.59).

Keywords: conducting materials · electrochemistry · fullerenes · photovoltaic devices · thiophenes

Introduction

Whilst functionalized fullerene derivatives are the most-promising electron-accepting materials in organic photovoltaic (OPV) devices, there is only a limited repertoire of such fullerene electron-acceptors. Only a few types of fullerene derivatives are known to be viable for application in OPV devices, including [6,6]-phenyl-C61-butyric acid methyl esters (PCBMs),[1,2] 1,4-dialkylfullerenes,[3] 1,4-diarylfullerenes,[4] bis-adducts, such as bis-PCBM[5] and indene C_{60} bis-adducts (ICBAs),[6] and methanofullerene derivatives.[7] Increased variety in fullerene-based acceptors has been widely pursued, because it would significantly expand the field of OPV research. This pursuit is not only limited to the improvement of power-conversion efficiency, but also includes fundamental research on morphology control[3e,8] and excited-state dynamics.[9]

Herein, we focus on 1,4-diadducts that contain one alkyl group and one aryl group (Scheme 1). In general, 1,4-dialkylfullerenes that contain insulating aliphatic groups usually exhibit low carrier mobility, with the exception of molecules such as 1,4-bis(dimethylphenylsilylmethyl)[60]fullerene (SIMEF),[3] which form columnar arrays of C_{60} cores that result in good electron mobility. On the other hand, 1,4-diarylfullerenes possess comparative electronic properties, but the rigidity of their aryl groups results in poorer solubility. Thus, our motivation has been to achieve a good balance between solubility and favorable electronic properties, which are conferred by the alkyl group and the aryl group, respec-

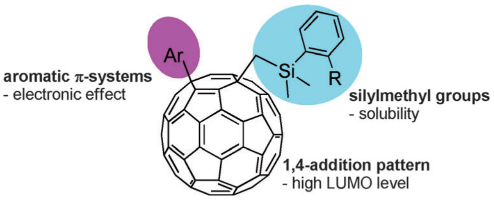

Scheme 1. Molecular design of the 1,4-diadducts.

---

[a] Prof. Dr. Y. Matsuo, H. Oyama, Dr. I. Soga, Dr. T. Okamoto,
Dr. H. Tanaka, Prof. Dr. E. Nakamura
Department of Chemistry, School of Science
The University of Tokyo
7-3-1 Hongo, Bunkyo-ku, Tokyo 113-0033 (Japan)
Fax: (+81) 3-5800-6889
E-mail: matsuo@chem.s.u-tokyo.ac.jp
nakamura@chem.s.u-tokyo.ac.jp

[b] Dr. I. Soga
Mitsubishi Chemical Group Science and
Technology Research Center, Inc.
1000 Kamoshida, Aoba-ku, Yokohama
Kanagawa 227-8502 (Japan)

[c] Dr. A. Saeki, Prof. Dr. S. Seki
Department of Applied Chemistry
Graduate School of Engineering
Osaka University
2-1 Yamadaoka, Suita, Osaka 565-0871 (Japan)

[d] Dr. T. Okamoto
Current address:
Department of Advanced Electron Devices
The Institute of Scientific and
Industrial Research (ISIR)
8-1 Mihogaoka, Ibaraki, Osaka 567-0047 (Japan)

tively. Moreover, because 1,4-diadducts have smaller π-conjugated systems than 1,2-diadducts, their LUMO levels are higher, thus resulting in a higher open-circuit voltage (V_{OC}) in OPV devices.[3]

Herein, we report the synthesis of 1-aryl-4-silylmethyl[60]fullerenes, including the characterization of their electrochemical properties, crystal-packing structures, and photovoltaic performance in OPV devices. An anisyl group and a thienyl group were chosen as the aryl groups because of their electron-donating nature, which was expected to raise the LUMO levels and to increase the V_{OC} value. The addition of a thienyl group to fullerene derivatives has previously been attempted to obtain fullerene–thiophene hybrids,[10] which were expected to exhibit properties of both fullerene and of the standard electron donor, poly(3-hexylthiophene) (P3HT). 1-Aryl-4-silylmethyl[60]fullerenes are regioisomers of 1-aryl-2-silylmethyl[60]fullerenes, which have been previously synthesized by the migration of aryl groups from the silicon side-chain to the fullerene core.[11] A respectable power-conversion efficiency of 3.4% was achieved herein, thus demonstrating that 1-aryl-4-silylmethyl[60]fullerenes can serve as viable electron-acceptors to produce efficient and competitive OPV devices.

Results and Discussion

Synthesis of 1,2-Arylhydro[60]fullerenes

In general, there are three methods to obtain mono(aryl)hydro[60]fullerenes. The first is a sulfoxide (DMSO)-assisted monoaddition reaction of an aryl Grignard reagent to C_{60},[3] the second is an $AlCl_3$-mediated Friedel–Crafts-type hydroarylation reaction,[12] and the third is a transition-metal-catalyzed arylation reaction of C_{60} by using arylboronic acids.[13] Herein, the first method was chosen. A previous report[1b] described only one example with a *p*-anisyl Grignard reagent and so we studied the scope and limitations of this reaction.

Abstract in Japanese:
C_{60}に１つのアリール基と１つのシリルメチル基を付加させて得られる1-アリール-4-シリルメチル[60]フラーレンを合成した．一段階目の反応として，ジメチルスルホキシドを添加剤として用いる高効率なアリールグリニャール試薬の求核付加を確立した．二段階目のハロゲン化シリルメチルとの求核置換反応は，1,4-位に位置選択的に進行した．X線結晶構造解析によるパッキング構造解析，時間分解マイクロ波伝導度測定，電子移動度測定により，アリール基として2-チエニル基を有する化合物が比較的良い物性をもつことがわかった．P3HTを用いたバルクヘテロ接合素子，テトラベンゾポルフィリンを用いたp-nヘテロ接合素子およびp-i-n接合素子の３種の有機薄膜太陽電池を作製し，フラーレン電子受容体の評価を行ったところ，2-チエニル誘導体がいずれの素子でも高い特性を与えた．また，1,4-付加形式に由来する高いLUMO準位に基づいて，高い開放電圧を与えた

We studied the DMSO-assisted monoaddition reaction with various aryl Grignard reagents, [Eq. (1)], including both electron-donating- and electron-withdrawing groups, to obtain compounds **1**–**5**. The addition reaction of electron-rich aryl groups, such as the anisyl and dimethyl amino groups, occurred more smoothly and more readily than that of electron-deficient aryl groups, such as the trifluoromethylphenyl group. We also included a 2-thienyl group to obtain a mono(thienyl)hydro[60]fullerene (**5**) in moderate yield. To our knowledge, compound **5**, a 2-substituted thienyl fullerene compound, is a new compound, although a 3-substituted regioisomer had been previously synthesized by a palladium-catalyzed hydroarylation reaction.[13b]

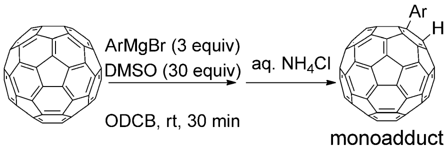

(1)

Ar	monoadduct yield (%)
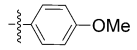	(**1**) 83
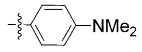	(**2**) 86
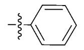	(**3**) 37
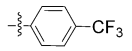	(**4**) 48
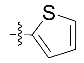 [a]	(**5**) 56

[a] Grignard reagent (6 equiv), DMSO (6 equiv)

Synthesis and Properties of 1-Aryl-4-silylmethyl[60]fullerenes

Next, we deprotonated compounds **1**–**5** with a base to obtain monoaryl[60]fullerene anions, which reacted with silylmethyl halides to give 1-aryl-4-silylmethyl[60]fullerenes **6**–**10** in 18–36% yield [Eq. (2)]. We investigated the solubility of the 1-aryl-4-silylmethyl[60]fullerene products in toluene, which is a commonly used solvent for device fabrication. The solubilities were in the range 0.3–0.9 wt.%, which are acceptable values for spin-coating processes.

The electrochemical properties of compounds **6**–**10** were investigated by cyclic voltammetry in THF. Cyclic voltammograms for all compounds exhibited three reversible one-electron-reduction waves (Figure 1). The LUMO levels of all of the compounds were calculated by using the equation: LUMO level = −(first reduction potential versus Fc/Fc^++4.8). Compounds with electron-donating groups on the aryl groups (compounds **6**, **7**, and **10**) showed a LUMO level that was approximately 0.1 eV higher than unsubstituted

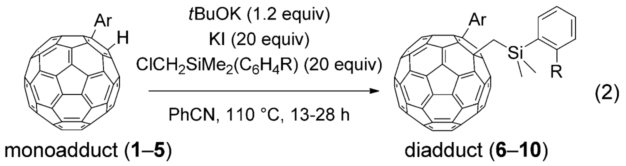

(2)

Ar	diadduct yield (%)	solubility in toluene (wt%)
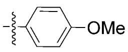	(**6a**: R = H) 21	0.4
	(**6b**: R = O*i*Pr) 36	0.8
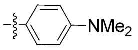	(**7**) 34	0.6
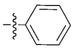	(**8**) 18	0.3
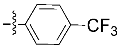	(**9**) 19	0.4
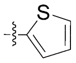 [a]	(**10a**: R = H) 24	0.5
	(**10b**: R = O*i*Pr) 28	0.9

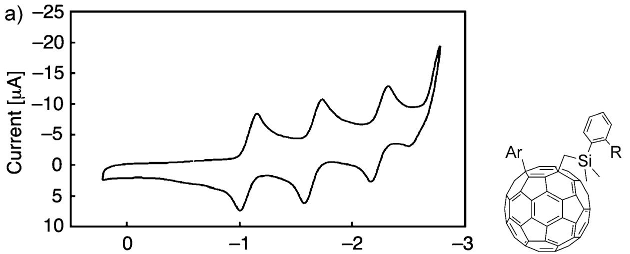

b)

Ar		LUMO (eV)	Ar		LUMO (eV)
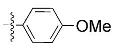	(**6a**)	–3.72	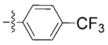	(**9**)	–3.86
	(**6b**)	–3.72			
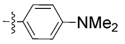	(**7**)	–3.72	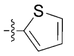 [a]	(**10a**)	–3.71
				(**10b**)	–3.71
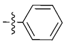	(**8**)	–3.81	PCBM		–3.80
			SIMEF		–3.74

LUMO level = –($E_{1/2}$ + 4.8)

Figure 1. Electrochemical data. a) Cyclic voltammogram of compound **6a**. b) Summarized LUMO levels of compounds **6**–**10**.

compound **8**. The introduction of an electron-withdrawing trifluoromethyl group (compound **9**) led to a relative decrease in the LUMO level by 0.05 V. On the other hand, the introduction of an electron-donating *o*-isopropoxy group onto the phenyl group on the silicon atom (compound **10b**) did not change the LUMO level.

Performance of the Photovoltaic Device

To determine the molecular structure of 1-aryl-4-silylmethyl[60]fullerenes and to examine the packing structure that influences carrier mobility (see below), we performed X-ray crystallography on single crystals of compounds **6a** and **10a** (Figure 2 and Figure 3). In the crystal-packing structure of compound **6a**, pairs of molecules associate through a fullerene–aryl-group π–π interaction in the manner as shown in Figure 2, upper right.[14,15] The distance between the fullerene moiety of one molecule and the aryl group of the other molecule is very short (3.17 Å; sum of van der Waals radii of the two carbon atoms: 3.4 Å). The pairs of molecules are arranged in a grid-like structure (Figure 2, bottom) with inter-fullerene distances of 3.38, 3.45, and 3.47 Å. The packing structure of thienylfullerene **10a** also showed fullerene–aryl-group interactions, with a thiophene–fullerene distance of 3.37 Å. The fullerene and thiophene moieties are arranged in an interpenetrating way along the *b* and *c* axes (Figure 3, bottom) to form anisotropic crystals. Inter-fullerene distances in the crystal of compound **10a** were 3.34 and 3.38 Å.

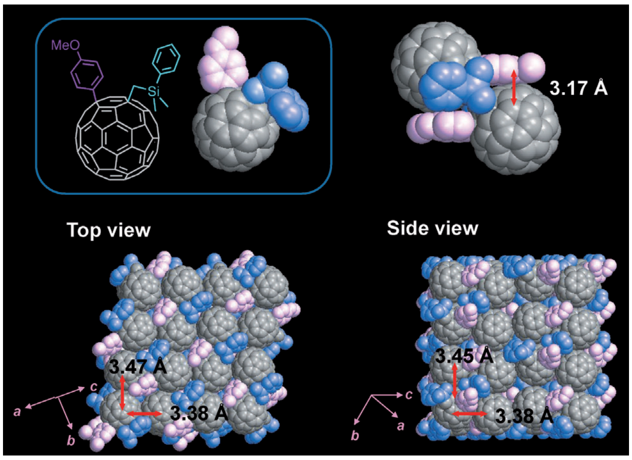

Figure 2. Crystal structure of compound **6a**; all molecules are depicted by using a space-filling model.

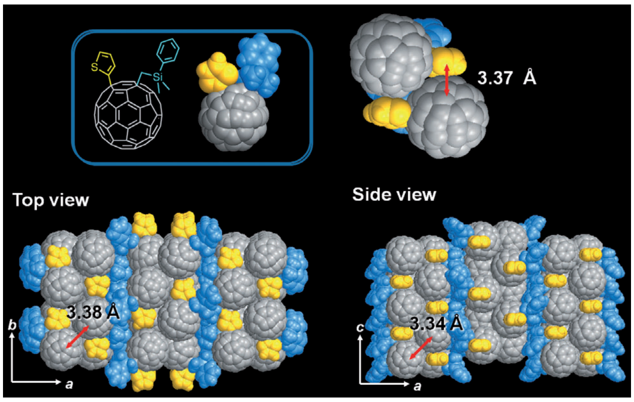

Figure 3. Crystal structure of compound **10a**; all molecules are depicted by using a space-filling model.

Photoconductivity and Carrier Mobility

Prior to the investigations of photovoltaic performance, we investigated the photoconductivity of blended films of compounds **6b** and **10b** with poly(3-hexylthiophene) (P3HT) by means of a flash-photolysis time-resolved microwave-conductivity (FP-TRMC) method (wavelength of the pulse laser: $\lambda = 515$ nm).[16] The TRMC method is an electrodeless measurement method that enables the determination of carrier mobility, photoconductivity, the quantum yield of carrier-generation, and the lifetime of generated carriers in micro-sized regions of organic thin-films. In this method, the microwave-absorption-mediated dielectric loss of carriers is measured by time-resolved microwave spectroscopy under the irradiation of a pulse-excitation laser.

The TRMC photoconductivity values of the blended films of compounds **6b** and **10b** with P3HT were $\phi\Sigma\mu = 3\times10^{-3}\,\mathrm{cm^2\,V^{-1}\,s^{-1}}$ and $5\times10^{-3}\,\mathrm{cm^2\,V^{-1}\,s^{-1}}$, respectively. We ascribe the higher photoconductivity of the P3HT:**10b** film to both the molecular structure and the supramolecular organization of compound **10b**. The conjugation between the electron-donating thiophene and the electron-accepting fullerene groups enables efficient carrier generation, whilst the closer packing of the fullerene cores permits efficient charge-transfer processes.

A comparative performance was also observed for compound **10b** in a space-charge-limited current (SCLC) mobility measurement. Because the SCLC electron mobility of compound **10b** ($5\times10^{-5}\,\mathrm{cm^2\,V^{-1}\,s^{-1}}$) was higher than that of compound **6b** ($1\times10^{-5}\,\mathrm{cm^2\,V^{-1}\,s^{-1}}$), we expected that the thienyl fullerene would show better performance in the photovoltaic application compared with the anisyl fullerene.

Photovoltaic Applications (Bulk Heterojunction)

Next, we evaluated the photovoltaic performance of 1-aryl-4-silylmethyl[60]fullerenes in which the aryl groups were *p*-anisyl and 2-thienyl groups. We employed *o*-isopropoxy-substituted compounds **6b** and **10b**, which had the best solubility in organic solvents; SIMEF and PCBM were used as reference materials. First, we fabricated standard bulk-heterojunction devices, which had an ITO/PEDOT:PSS/P3HT:fullerene-derivative/NBphen/Al structure (Figure 4). The device with 2-thienyl fullerene **10b** recorded a power-conversion efficiency (PCE) of 2.8% ($V_{OC} = 0.61$ V, short-circuit current density (J_{SC}): 8.7 mA cm^{-2}, fill factor (*FF*): 0.53). Although the efficiency was lower than those of devices that used the standard reference materials, SIMEF (3.6%) and PCBM (3.2%), this value is respectable when compared with other P3HT-based bulk-heterojunction devices. Furthermore, the device with compound **10b** showed a higher V_{OC} compared to that with PCBM ($V_{OC} = 0.55$ V). This result was attributed to the higher-lying LUMO level (−3.71 eV vs. −3.80 eV for PCBM) of compound **10b**, which was derived from a 1,4-addition pattern and the electron-donating thienyl group.

On the other hand, the device with *p*-anisyl fullerene **6b** gave low J_{SC} (1.7 mA cm^{-2}) and *FF* values (0.36), thereby leading to a low PCE of 0.38%. The lower performance of the P3HT:**6b** OPV device was in good agreement with the poorer TRMC photoconductivity that was exhibited by the blended film that comprised P3HT and compound **6b**.

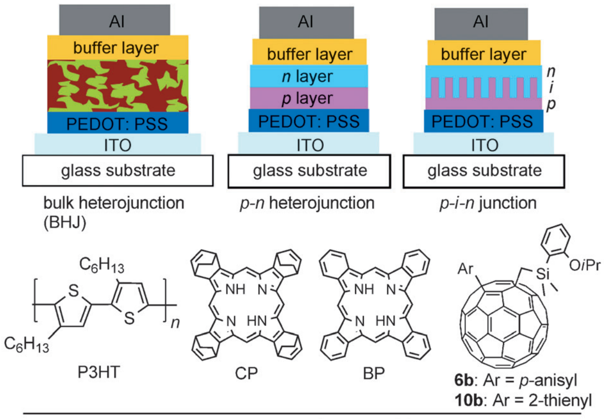

acceptor	donor	structure	J_{SC} [mA/cm^2]	V_{OC} [V]	*FF*	PCE [%]
6b	P3HT	BHJ	1.7	0.62	0.36	0.38
10b	P3HT	BHJ	8.7	0.61	0.53	2.8
SIMEF	P3HT	BHJ	9.0	0.65	0.62	3.6
PCBM	P3HT	BHJ	9.2	0.55	0.63	3.2
6b	BP	*p-n*	6.3	0.66	0.63	2.3
10b	BP	*p-n*	6.8	0.66	0.61	2.7
6b	BP	*p-i-n*	7.2	0.71	0.56	2.8
10b	BP	*p-i-n*	8.1	0.69	0.59	3.4

Figure 4. Structure and obtained performance of OPV cells by using fullerene derivatives (compounds **6b** and **10b**, as well as reference compounds SIMEF and PCBM).

Photovoltaic Applications (*p–n* Heterojunction)

Next, we examined compounds **6b** and **10b** for use in small-molecule OPV devices by using tetrabenzoporphyrin (BP) as a donor (Figure 4); BP was obtained from a soluble precursor material (CP) through a thermally induced retro-Diels–Alder reaction.[17] CP is solution-processable and thin-films of CP can be converted into insoluble crystalline thin films of BP by heating. Subsequently, acceptor materials can be deposited onto the BP layer by solution processing. The BP layers for each obtained device possessed the same organization structure and, thus, had the same interfacial structure. This result allowed us to evaluate the intrinsic electronic performance of the acceptor materials without the influence of morphology.

A solution of CP in a mixture of $CHCl_3$ and chlorobenzene (1:2, v/v) was spin-coated on a PEDOT:PSS layer that was coated on ITO glass. The substrate was heated at 180 °C for 20 min to obtain a BP (*p*) layer. A solution of either compound **6b** or **10b** (0.7 wt.%) in a mixture of chlorobenzene and CS_2 (1:1, v/v) was then spin-coated on top of the *p* layer to form an *n* layer, thus giving a solution-processed *p–n* heterojunction device. The device was then thermally annealed at 120 °C for 5 min. The fabricated OPV devices with a *p–n* junction that were formed by using compounds **6b** and **10b** exhibited PCEs of 2.3% and 2.7%, respectively. As with the bulk-heterojunction devices, a higher PCE was obtained for the 2-thienyl compound (**10b**), thus leading to the conclusion that the 2-thienyl compound **10b** is superior to *p*-anisyl compound **6b** in its fundamental electronic properties.

Photovoltaic Applications (*p*–*i*–*n* Junction)

Finally, we fabricated devices with a *p*–*i*–*n* junction that had a bulk-heterojunction interlayer (*i* layer) between the donor (*p*) and acceptor (*n*) layers (Figure 4). Fabrication of the *i* layer was achieved through a solution process, with the use of a tetrabenzoporphyrin precursor, CP.[3b] After the fabrication of insoluble BP *p* layers, solutions of CP and the fullerene derivatives (**6b** or **10b**) were spin-coated onto the *p* layer. After heating the substrate to convert CP into BP in the *i* layer, subsequent spin-coating of the respective fullerene derivatives formed the *n* layers, thereby affording *p*–*i*–*n* junctions.

The *p*–*i*–*n* devices with compounds **6b** and **10b** showed PCE values of 2.8% and 3.4%, respectively, which were higher than those of their corresponding *p*–*n* devices. Similar to polymer-based bulk-heterojunction devices and small-molecule-based devices with a *p*–*n* heterojunction (see above), 2-thienyl compound **10b** performed better than compound **6b**. In comparison with the devices with a *p*–*n* heterojunction, the J_{SC} value was improved from approximately 6–7 mA cm^{-2} to 7–8 mA cm^{-2}, presumably because of an increase in the film-thickness of the *p*–*i*–*n* devices. In general, *p*–*i*–*n* devices retain their effectiveness, even when thicker films are used, because the interpenetrating *i* layer enables the efficient utilization of the photogenerated excitons. On the other hand, a BP:PCBM device with a similar *p*–*i*–*n* junction only achieved a PCE of 2.0%.[3b] The respectable performance of the devices with compounds **6b** and **10b** indicates that there is significant potential for the use of 1,4-thienyl-alkyl fullerenes in the research of device-structure-modification on OPV cells.

Conclusions

We have described a method for the synthesis of 1-aryl-4-silylmethyl[60]fullerenes (aryl = *p*-anisyl, *p*-dimethylaminophenyl, phenyl, *p*-trifluoromethylphenyl, and 2-thienyl), new types of 1,4-diadducts, which possess relatively high-lying LUMO levels and tunable aryl groups that control the packing structures. During the synthesis of the target compounds, an efficient DMSO-assisted installation of a 2-thienyl group on fullerene was found to produce a key intermediate compound. 1-Aryl-4-silylmethyl[60]fullerenes that contained anisyl and thienyl groups were characterized by X-ray crystallography, photoconductivity experiments, and by the fabrication of solution-processed OPV devices. The 2-thienyl compounds were superior to the *p*-anisyl compounds in terms of both their crystal-packing structure and the TRMC photoconductivity of the blended film that was composed of P3HT and fullerenes. The evaluation of OPV devices with a bulk heterojunction, *p*–*n* heterojunction, and a *p*–*i*–*n* junction yielded similar observations: the thienyl fullerene (**10b**) exhibited better performance than the anisyl one (**6b**). Nevertheless, both types of compounds were found to be suitable for the solution-processing-based fabrication of OPVs because of the high solubility that was conferred by the silylmethyl group. The 3.4% PCE that was obtained was respectable, which suggests that these 1-aryl-4-silylmethyl[60]fullerenes, especially those that have a thienyl group as an aryl moiety, are promising fullerene electron acceptors for applications as OPV devices. Optimization of the donor materials and device structures will also provide further opportunities to produce efficient OPV devices.

Experimental Section

General

All manipulations were carried out under an argon atmosphere by using standard Schlenk techniques. KO*t*Bu and (trimethylsilyl)methyl triflate were purchased from Aldrich and used as received without further purification. KI was purchased from Wako and heated at 100°C before use. All anhydrous organic solvents were purchased from Kanto chemicals and purified by a solvent purification system (GlassContour) that was equipped with columns of activated alumina and a supported copper catalyst (G-5) before use. Column chromatography on silica gel was performed on Kanto Silica gel 60 (spherical, neutral, 140–325 mesh). NMR spectra were measured on JEOL, ECX-400, and ECA-500 spectrometers and reported in parts per million (ppm) relative to tetramethylsilane ($\delta = 0.00$ ppm). ^{1}H NMR spectra were recorded in either $CDCl_3$ or in a mixture of $CDCl_3$ and CS_2 and were referenced internally to tetramethylsilane as a standard; ^{13}C NMR spectra were referenced to the solvent resonance. Methyl-, methylene-, and methine signals in the ^{13}C NMR spectra were assigned by DEPT spectra. HPLC analysis was performed on a Shimadzu LC-10A system that was equipped with a SPD-M10A diode-array detector and a Cosmosil-Buckyprep column (4.6×250 mm, Nacalai Tesque Co.). Atmospheric pressure chemical ionization (APCI)-HRMS was measured on a JEOL JMS-T100 LC ESI-TOF mass spectrometer.

$C_{60}(C_6H_4{-}OMe)H$ (**1**)

A solution of $4\text{-}MeOC_6H_4MgBr$ (1.89 mL, 1.10 M, 2.08 mmol) in THF was added to a solution of C_{60} (500 mg, 0.694 mmol) in 1,2-dichlorobenzene (150 mL) that contained DMSO (1.48 mL, 20.83 mmol) at 25°C. The color of the solution immediately changed from purple to dark green. After stirring for 30 min, a saturated aqueous solution of NH_4Cl (1.0 mL) was added to stop the reaction. The resulting dark-red solution was subjected to vacuum distillation to remove the 1,2-dichlorobenzene. The residue, which contained a small amount of 1,2-dichlorobenzene (about 0.5–3 mL), was dissolved in toluene (200 mL) and passed through a pad of silica gel to remove the magnesium salts. The mixture was concentrated to obtain a solution (about 5–10 mL) that contained the product. Purification of the product by column chromatography on silica gel (CS_2/*n*-hexane, 1:1 to 2:1) afforded the title compound (477 mg, 0.576 mmol, 83% yield) as black crystals. ^{1}H NMR (500 MHz, $CDCl_3/CS_2$): $\delta = 3.98$ (s, 3H), 6.72 (s, 1H), 7.27–7.29 (m, 2H), 8.34–8.37 ppm (m, 2H); ^{13}C NMR (500 MHz, $CDCl_3/CS_2$): $\delta = 55.34$, 63.86, 67.3, 115.22, 128.71, 128.72, 135.00, 135.69, 136.31, 140.23, 140.29, 140.54, 141.17, 141.58, 141.65, 141.97, 142.02, 142.04, 142.31, 142.56, 142.57, 143.28, 144.56, 144.65, 144.73, 145.38, 145.41, 145.49, 145.51, 145.81, 145.93, 146.18, 146.20, 146.35, 146.40, 146.85, 147.27, 147.51, 152.65, 154.14, 159.32 ppm; HRMS (APCI−): *m*/*z* calcd for $C_{67}H_8O$: 829.0575 $[M]^-$; found: 829.0616.

$C_{60}(C_6H_4{-}NMe_2)H$ (**2**)

The procedure described for compound **1** was performed by using 4-$(Me_2N){-}C_6H_4MgBr$ in place of $4\text{-}MeOC_6H_4MgBr$ to obtain compound **2**

(20.2 mg, 0.024 mmol, 86 %) as black crystals. ^{1}H NMR (400 MHz, $CDCl_3/CS_2$): $\delta = 3.17$ (s, 6 H), 6.75 (s, 1 H), 7.07–7.10 (m, 2 H), 8.24–8.27 ppm (m, 2 H); ^{13}C NMR (400 MHz, $CDCl_3/CS_2$): $\delta = 29.92$, 40.51, 63.80, 67.27, 113.50, 128.15, 135.52, 136.41, 140.18, 140.22, 141.52, 141.62, 141.20, 142.03, 142.34, 142.49, 142.53, 143.23, 144.58, 144.62, 145.33, 145.35, 145.38, 145.48, 145.81, 146.09, 146.12, 146.15, 146.28, 146.36, 146.86, 147.23, 147.44, 149.84, 152.84, 154.62 ppm; HRMS (APCI−): *m*/*z* calcd for $C_{68}H_{11}N$: 842.0891 $[M]^-$; found: 842.0900.

*$C_{60}(C_6H_5)H$ (**3**)*

The procedure described for compound **1** was performed by using C_6H_5MgBr in place of $4\text{-}MeOC_6H_4MgBr$ to obtain compound **3** (205 mg, 0.257 mmol, 37 %) as black crystals. ^{1}H NMR (500 MHz, $CDCl_3/CS_2$): $\delta =$ 6.73 (s, 1 H), 7.08–7.11 (m, 2 H), 7.22–7.25 (m, 1 H), 7.28–7.31 ppm (m, 2 H); ^{13}C NMR (500 MHz, $CDCl_3/CS_2$): $\delta = 63.86$, 66.54, 113.22, 128.31, 128.82, 128.94, 135.51, 136.62, 140.23, 140.29, 141.52, 141.61, 141.98, 142.03, 142.35, 142.48, 142.55, 143.31, 144.56, 144.62, 145.32, 145.35, 145.40, 145.47, 145.82, 146.09, 146.12, 146.15, 146.27, 146.36, 146.86, 147.07, 147.34, 149.85, 152.08 ppm; HRMS (APCI−): *m*/*z* calcd for $C_{66}H_6$: 799.0470 $[M]^-$; found: 799.04900.

*$C_{60}(C_6H_4CF_3)H$ (**4**)*

The procedure described for compound **1** was performed by using 4-FC_6H_4MgBr in place of $4\text{-}MeOC_6H_4MgBr$ to obtain compound **4** (173 mg, 0.120 mmol, 48 %) as black crystals. ^{1}H NMR (500 MHz, $CDCl_3$): $\delta = 7.04$ (s, 1 H), 7.94–7.96 (d, $J = 8.3$ Hz, 2 H), 8.47–8.49 ppm (d, $J = 8.3$ Hz, 2 H); ^{13}C NMR (500 MHz, $CDCl_3/CS_2$): $\delta = 63.58$, 65.43, 114.22, 128.77, 128.73, 135.42, 135.66, 140.18, 140.27, 141.51, 141.62, 141.65, 141.99, 142.03, 142.04, 142.53, 143.22, 143.57, 144.57, 144.62, 145.33, 145.34, 145.41, 145.47, 145.49, 145.81, 146.08, 146.13, 146.35, 146.43, 146.75, 147.27, 147.23, 147.77, 151.45, 154.16, 154.62 ppm; HRMS (APCI−): *m*/*z* calcd for $C_{67}H_5F_3$: 867.0343 $[M]^-$; found: 867.0359.

*$C_{60}(C_4H_3S)H$ (**5**)*

A solution of $(C_4H_3S)MgBr$ (5.37 mL, 0.85 M, 4.58 mmol) in THF was added to a solution of C_{60} (550 mg, 0.764 mmol) in 1,2-dichlorobenzene (150 mL) that contained DMSO (0.33 mL, 4.58 mmol) at 25 °C. The color of the solution gradually changed from purple to dark green. After stirring for 48 h, a saturated aqueous solution of NH_4Cl (1.0 mL) was added to stop the reaction. The resulting dark-red solution was subjected to vacuum distillation to remove the 1,2-dichlorobenzene. The residue, which contained a small amount of 1,2-dichlorobenzene (about 0.5–3 mL) was dissolved in toluene (200 mL) and passed through a pad of silica gel to remove the magnesium salts. The mixture was concentrated to obtain a solution (about 5–10 mL) that contained the product. Purification of the product by column chromatography on silica gel (CS_2/*n*-hexane, 1:1 to 1:0) afforded the title compound (477 mg, 0.576 mmol, 56 % yield) as black crystals. ^{1}H NMR (500 MHz, $CDCl_3/CS_2$): $\delta = 6.95$ (s, 1 H), 7.20–7.26 (m, 1 H), 7.63–7.65 (dd, 1 H), 7.92–7.93 ppm (dd, 1 H); ^{13}C NMR (500 MHz, $CDCl_3/CS_2$): $\delta = 63.68$, 65.44, 103.77, 125.80, 126.11, 127.89, 133.33, 135.25, 136.31, 136.84, 140.23, 140.29, 140.32, 140.33, 140.54, 141.62, 141.65, 142.07, 142.60, 143.02, 143.24, 145.49, 145.51, 145.81, 144.69, 145.62, 146.19, 146.22, 146.35, 146.42, 146.72, 148.54, 151.95, 153.31 ppm; HRMS (APCI−): *m*/*z* calcd for $C_{64}H_4S$: 805.0034 $[M]^-$; found: 805.0054.

*$C_{60}(C_6H_4\text{–}OMe)(CH_2Si(Me)_2Ph)$ (**6a**)*

A solution of KO*t*Bu (0.184 mL, 1.0 M, 0.184 mmol) in THF (1.0 M) was added to a solution of compound **1** (76.0 mg, 0.0918 mmol) in PhCN at 25 °C. A dark-green solution of the potassium salt of compound **1** was immediately obtained. After stirring for 30 min, $PhSi(Me)_2CH_2Cl$ (0.33 mL, 1.86 mmol) and potassium iodide (0.305 g, 1.86 mmol) were added to the solution. After stirring for 18 h at 110 °C, a saturated aqueous solution of NH_4Cl (1.0 mL) was added to stop the reaction. Evaporation of volatile compounds gave crude product **6a**. Purification of the product by column chromatography on silica gel (CS_2/*n*-hexane, 1:4 to 1:1) and by preparative HPLC (Buckyprep column; eluent: toluene/2-propanol, 6:4) afforded the title compound (18.8 mg, 0.0193 mmol, 21 % yield) as black crystals. ^{1}H NMR (500 MHz, $CDCl_3/CS_2$): $\delta = 0.60$ (s, 3 H), 0.64 (s, 3 H), 2.55 (d, $J = 14.6$ Hz, 1 H), 2.71 (d, $J = 14.6$ Hz, 1 H), 3.95 (s, 3 H), 7.16–7.17 (m, 2 H), 7.30–7.32 (m, 3 H), 7.57–7.59 (m, 2 H), 8.11–8.10 ppm (m, 2 H); ^{13}C NMR (500 MHz, $CDCl_3/CS_2$): $\delta = 21.91$, 22.06, 29.77, 30.47, 55.35, 68.66, 110.17, 114.85, 119.86, 123.55, 125.62, 128.31, 128.71, 128.72, 131.38, 133.26, 134.17, 135.03, 135.69, 136.18, 136.31, 140.23, 140.29, 140.54, 140.58, 141.17, 141.23, 141.58, 141.65, 141.97, 142.02, 142.04, 142.11, 142.31, 142.56, 142.57, 142.93, 143.28, 143.59, 144.26, 144.31, 144.35, 144.54, 144.56, 144.65, 144.72, 144.73, 145.38, 145.41, 145.49, 145.51, 145.81, 145.93, 146.15, 146.18, 146.20, 146.28, 146.35, 146.36, 146.40, 146.67, 146.86, 147.27, 147.51, 147.82, 148.63, 154.14, 154.37, 157.47, 158.90, 159.49 ppm; HRMS (APCI−): *m*/*z* calcd for $C_{76}H_{20}SiO$: 977.1283 $[M]^-$; found: 977.1330.

*$C_{60}(C_6H_4\text{–}NMe_2)(CH_2Si(Me)_2Ph)$ (**7**)*

The procedure described for compound **6a** was performed by using compound **2** in place of compound **1** to obtain compound **7** (205 mg, 0.257 mmol, 37 %) as black crystals. ^{1}H NMR (500 MHz, $CDCl_3/CS_2$): $\delta =$ 0.56 (s, 3 H), 0.58 (s, 1 H), 2.51 (d, $J = 14.6$ Hz, 1 H), 2.81 (d, $J = 14.7$ Hz, 1 H), 3.05 (s, 6 H), 6.94–6.95 (m, 2 H), 7.27–7.28 (m, 3 H), 7.56–7.58 (m, 2 H), 8.00–8.02 ppm (m, 2 H); ^{13}C NMR (500 MHz, $CDCl_3/CS_2$): $\delta = 21.95$, 22.16, 29.76, 30.50, 55.35, 68.66, 110.14, 114.84, 117.26, 123.52, 125.66, 128.32, 131.71, 131.72, 134.17, 136.18, 135.69, 136.18, 136.31, 140.23, 140.29, 140.54, 140.58, 141.17, 141.23, 141.58, 141.65, 141.97, 142.02, 142.04, 142.11, 142.31, 142.56, 142.57, 142.93, 143.28, 143.59, 144.26, 144.31, 144.35, 144.54, 144.56, 144.65, 144.72, 144.73, 145.38, 145.41, 145.49, 145.51, 145.81, 145.93, 146.15, 146.19, 146.22, 146.27, 146.32, 146.36, 146.40, 146.67, 146.86, 146.93, 147.21, 147.59, 147.85, 148.65, 154.44, 154.36, 157.56, 158.79, 158.88 ppm; HRMS (APCI−): *m*/*z* calcd for $C_{77}H_{23}SiN$: 990.1600 $[M]^-$; found: 990.1624.

*$C_{60}(C_6H_5)(CH_2Si(Me)_2Ph)$ (**8**)*

The procedure described for compound **6a** was performed by using compound **3** in place of compound **1** to obtain compound **7** (102 mg, 0.128 mmol, 18 %) as black crystals. ^{1}H NMR (500 MHz, $CDCl_3/CS_2$): $\delta =$ 0.65 (s, 3 H), 0.66 (s, 3 H), 2.55 (d, $J = 14.6$ Hz, 1 H), 2.71 (d, $J = 14.6$ Hz, 1 H), 7.25–7.27 (m, 2 H), 7.29–7.31 (m, 4 H), 7.52–7.53 (m, 1 H), 7.60–7.62 (m, 2 H), 7.64–7.66 ppm (m, 1 H); ^{13}C NMR (500 MHz, $CDCl_3/CS_2$): $\delta =$ 22.01, 22.04, 29.77, 30.47, 55.35, 68.66, 110.17, 114.85, 119.86, 123.55, 125.62, 128.31, 128.71, 128.72, 131.38, 133.26, 134.17, 135.03, 135.69, 136.18, 136.31, 140.23, 140.29, 140.54, 140.58, 141.17, 141.23, 141.58, 141.65, 141.97, 142.02, 142.04, 142.11, 142.31, 142.56, 142.57, 142.93, 143.28, 143.59, 144.26, 144.31, 144.35, 144.54, 144.56, 144.65, 144.72, 144.73, 145.38, 145.41, 145.49, 145.51, 145.81, 145.93, 146.15, 146.18, 146.20, 146.28, 146.35, 146.36, 146.40, 146.67, 146.86, 147.27, 147.59, 147.82, 148.58, 148.72, 149.43, 149.55, 154.52, 155.26, 158.00, 158.03 ppm; HRMS (APCI−): *m*/*z* calcd for $C_{75}H_{18}Si$: 947.1178 $[M]^-$; found: 947.1206.

*$C_{60}(C_6H_4\text{–}CF_3)(CH_2Si(Me)_2Ph)$ (**9**)*

The procedure described for compound **6a** was performed by using compound **4** in place of compound **1** to obtain compound **9** (11.0 mg, 0.190 mmol, 19 %) as black crystals. ^{1}H NMR (500 MHz, $CDCl_3/CS_2$): $\delta =$ 0.51 (s, 3 H), 0.57 (s, 3 H), 2.53 (d, $J = 14.6$ Hz, 1 H), 2.73 (d, $J = 14.6$ Hz, 1 H), 7.26–7.29 (m, 2 H), 7.31–7.34 (m, 4 H), 7.52–7.53 (m, 1 H), 7.57–7.59 (m, 2 H), 7.64–7.66 ppm (m, 1 H); ^{13}C NMR (500 MHz, $CDCl_3/CS_2$): $\delta =$ 22.87, 27.66, 29.77, 29.93, 55.37, 69.25, 110.17, 114.85, 119.86, 123.55, 125.62, 128.31, 128.71, 128.72, 131.38, 133. 26, 134.17, 135.03, 135.69, 136.18, 136.31, 140.23, 140.29, 140.54, 140.58, 141.17, 141.23, 141.58, 141.65, 141.97, 142.02, 142.04, 142.11, 142.31, 142.56, 142.57, 142.93, 143.28, 143.59, 144.35, 144.59, 144.63, 144.67, 144.91, 144.96, 144.98, 145.30, 145.34, 145.49, 146.70, 146.72, 146.81, 146.84, 147.02, 147.05, 147.13, 147.53, 147.76, 147.99, 148.45, 148.46, 148.72, 151.20, 154.23, 157.65, 158.25 ppm; HRMS (APCI−): *m*/*z* calcd for $C_{76}H_{17}SiF_3$: 1015.1052 $[M]^-$; found: 1015.1084.

$C_{60}(C_4H_3S)(CH_2Si(Me)_2Ph)$ (**10a**)

The procedure described for compound **6a** was performed by using compound **5** in place of compound **1** to obtain compound **10a** (24 % yield) as black crystals. ^{1}H NMR (500 MHz, $CDCl_3/CS_2$): $\delta = 0.64$ (s, 3 H), 0.67 (s, 3 H), 2.55 (d, $J = 14.6$ Hz, 1 H), 2.71 (d, $J = 14.6$ Hz, 1 H), 7.25–7.27 (m, 2 H), 7.29–7.31 (m, 4 H), 7.52–7.53 (m, 1 H), 7.60–7.62 (m, 2 H), 7.64–7.66 ppm (m, 1 H); ^{13}C NMR (500 MHz, $CDCl_3/CS_2$): $\delta = 29.77$, 30.47, 55.35, 68.66, 111.14, 115.85, 118.53, 122.34, 124.92, 125.11, 128.31, 128.72, 133.38, 133.46, 135.17, 135.44, 135.49, 135.68, 136.31, 140.23, 140.29, 140.54, 140.58, 141.17, 141.23, 141.58, 141.65, 141.97, 142.02, 142.04, 142.11, 142.31, 142.56, 142.57, 142.93, 143.28, 143.59, 144.26, 144.31, 144.35, 144.54, 144.56, 144.65, 144.72, 144.73, 145.38, 145.41, 145.49, 145.51, 145.81, 145.93, 146.15, 146.16, 146.24, 146.30, 146.32, 146.39, 146.40, 146.65, 146.88, 147.63, 147.78, 147.92, 149.73, 154.06, 154.32, 157.34 ppm; HRMS (APCI−): m/z calcd for $C_{73}H_{16}SiS$: 953.0742 $[M]^-$; found: 953.0763.

$C_{60}(C_6H_4{-}OMe)(CH_2Si(Me)_2C_6H_4{-}OiPr)$ (**6b**)

A solution of KO*t*Bu (0.899 mL, 1.0 M, 0.899 mmol) in THF (1.0 M) was added to a solution of compound **1** (372.3 mg, 0.450 mmol) in PhCN at 25 °C. A dark-green solution of the potassium salt of compound **1** was immediately obtained. After stirring for 30 min, $(2\text{-}i\text{PrOC}_6H_4)Si(Me)_2CH_2Cl$ (1.61 mL, 8.99 mmol) and potassium iodide (1.49 g, 8.99 mmol) were added to the solution. After stirring for 18 h at 110 °C, a saturated aqueous solution of NH_4Cl (1.0 mL) was added to stop the reaction. Evaporation of volatile compounds gave the crude product. Purification by column chromatography on silica gel (CS_2/*n*-hexane, 1:1) and preparative HPLC (Buckyprep column; eluent: toluene/2-propanol, 6:4) afforded the title compound (177 mg, 0.162 mmol, 36 % yield) as black crystals. ^{1}H NMR (500 MHz, $CDCl_3/CS_2$): $\delta = 0.50$ (s, 3 H), 0.55 (s, 3 H), 1.17 (d, $J = 6.3$ Hz, 3 H), 1.25 (d, $J = 6.3$ Hz, 3 H), 2.58 (d, $J = 14.3$ Hz, 1 H), 2.71 (d, $J = 14.3$ Hz, 1 H), 3.90 (s, 3 H), 4.41 (m, 1 H), 6.56–6.58 (d, 1 H), 6.74–6.76 (t, 1 H), 7.13–7.14 (m, 2 H), 7.35–7.36 (m, 2 H), 8.15–8.17 ppm (m, 2 H); ^{13}C NMR (500 MHz, $CDCl_3/CS_2$): $\delta = 21.91$, 22.06, 29.77, 30.47, 55.35, 68.66, 110.17, 114.85, 119.86, 123.55, 125.62, 128. 31, 128.71, 128.72, 131.38, 133.26, 134.17, 135.03, 135.69, 136.18, 136.31, 140.23, 140.29, 140.54, 140.58, 141.17, 141.23, 141.58, 141.65, 141.97, 142.02, 142.04, 142.11, 142.31, 142.56, 142.57, 142.93, 143.28, 143.59, 144.26, 144.31, 144.35, 144.54, 144.56, 144.65, 144.72, 144.73, 145.38, 145.41, 145.49, 145.51, 145.81, 145.93, 146.15, 146.18, 146.20, 146.28, 146.35, 146.36, 146.40, 146.67, 146.86, 147.27, 147.51, 147.82, 148.63, 154.14, 154.37, 157.47, 158.90, 159.49 ppm; HRMS (APCI−): m/z calcd for $C_{85}H_{26}SiO$: 1091.1753 $[M]^-$; found: 1091.1176.

$C_{60}(C_4H_3S)(CH_2Si(Me)_2C_6H_4{-}OiPr)$ (**10b**)

The procedure described for compound **6b** was performed by using compound **5** in place of compound **1** to obtain compound **10b** (28 % yield) as black crystals. ^{1}H NMR (500 MHz, $CDCl_3/CS_2$): $\delta = 0.54$ (s, 3 H), 0.56 (s, 3 H), 1.24 (d, $J = 6$ Hz, 3 H), 1.31 (d, $J = 6$ Hz, 3 H), 2.62 (d, $J = 17.2$ Hz, 1 H), 2.75 (d, $J = 17.2$ Hz, 1 H), 3.94 (s, 3 H), 4.46 (m, 1 H), 6.59–6.61 (d, 2 H), 6.76–6.77 (t, 1 H), 7.17–7.19 (m, 2 H), 7.23–7.38 (m, 1 H), 8.17–8.19 ppm (m, 2 H); ^{13}C NMR (400 MHz, $CDCl_3/CS_2$): $\delta = 21.89$, 22.08, 30.69, 53.14, 56.35, 68.62, 110.06, 110.60, 114.85, 115.07, 116.28, 119.86, 119.96, 122.59, 125.56, 125.68, 127.51, 130.62, 131.37, 136.31, 136.53, 137.81, 139.38, 140.22, 140.26, 140.29, 140.43, 140.58, 140.61, 141.10, 141.13, 141.58, 141.62, 141.65, 141.96, 142.01, 142.04, 142.09, 143.43, 143.59, 143.94, 144.15, 144.26, 144.31, 144.73, 145.27, 145.38, 145.41, 145.81, 145.93, 146.15, 146.18, 146.20, 146.28, 146.35, 146.36, 146.59, 146.67, 146.74, 146.86, 147.27, 147.31, 147.51, 147.62, 147.64, 148.00, 148.63, 154.08, 154.15, 154.37, 157.47, 158.42, 159.39 ppm; HRMS (APCI−): m/z calcd for $C_{76}H_{22}SiSO$: 1011.1161 $[M]^-$; found: 1011.0079.

Electrochemical Measurements

Electrochemical measurements were performed on a Hokuto DenkoHZ-5000 voltammetric analyzer. A glassy carbon electrode, a platinum coil, and a Ag/Ag^+ electrode were used as the working electrode, the counter electrode, and the reference electrode, respectively. Cyclic voltammetry (CV) was performed at a scan rate of 100 mV s^{-1}. The potential was corrected against Fc/Fc^+.

X-ray Crystallographic Analysis

Single crystals of compounds **6a** and **10a** that were suitable for X-ray analysis were obtained by the slow diffusion of EtOH into solutions of compounds **6a** and **10a** in CS_2. X-ray crystallographic measurements were performed on a Rigaku R-AXIS RAPID II (imaging plate detector) by using graphite-monochromated $Cu_{K\alpha}$ radiation ($\lambda = 1.5405$ Å). The positional- and thermal parameters were refined by using the full-matrix least-squares method with the SHELXL97 program.

CCDC 895606 (**6a**) and CCDC 895605 (**10a**) contain the supplementary crystallographic data for this paper. These data can be obtained free of charge from The Cambridge Crystallographic Data Centre via www.ccdc.cam.ac.uk/data_request/cif.

FP-TRMC Measurements

Samples for flash-photolysis time-resolved microwave-conductivity (FP-TRMC) measurements were prepared by drop-casting blended solutions that contained P3HT (0.5 wt. % in chlorobenzene) and the corresponding fullerene derivative (**6a**: 0.25 wt. % in chlorobenzene; **10a**: 0.5 wt. % in chlorobenzene) onto UV/O_3-pretreated quartz substrates. These drop-cast films were thermally annealed at 120 °C for 10 min.

FP-TRMC measurements were carried out at 25 °C in air, where the resonant frequency and microwave power were properly adjusted to 9.1 GHz and 3 mW, respectively. Charge carriers were photochemically generated by using a 515 nm light pulse from an optical parametric oscillator (OPO) that was equipped with a Spectra-Physics model INDI Nd:YAG laser with a pulse duration of 5–8 ns. The excitation photon density was $3.8 \times 10^{15}/(\text{cm}^2 \text{ pulse})$. Transient conductivities ($\Delta\sigma$) were evaluated according to: $\Delta\sigma = (1A)(\Delta Pr/Pr)$, where A, ΔP_r, and P_r represent the sensitivity factor, the change in reflected microwave power, and the reflected microwave power, respectively. Subsequently, $\Delta\sigma$ was converted into the product of the quantum yield (ϕ) and the sum of charge-carrier mobilities, $\Sigma\mu = (\mu_h + \mu_e)$, according to $\phi\Sigma\mu = \Delta\sigma(eI_0F_{\text{light}})^{-1}$, where e, I_0, and F_{light} are the unit charge of a single electron, the incident photon density of the excitation laser (photons m^{-2}), and a correction (or filling) factor (m^{-1}), respectively.

SCLC Measurements (Determination of Electron Mobility)

The single-layered cells were prepared on ITO-coated glass substrates that were provided by GEOMATEC. ITO substrates were treated with UV/O_3 prior to spin-coating onto PEDOT:PSS. The PEDOT:PSS-coated substrate was dried in air at 120 °C for 10 min, then dried in a nitrogen glove box at 180 °C for 3 min prior to use. Subsequently, the fullerene derivative was spin-coated from a chlorobenzene/CS_2 (1:1) solution and was thermally annealed at 120 °C for 10 min. For the top electrode, 0.5 nm-thick LiF and 80 nm-thick Al were deposited. The J–V curves were measured by a computer-controlled Keithley 2400 source meter. The electron mobility was determined by fitting to a space-charge-limited-current (SCLC). The SCLC is given by $J = (9/8)\varepsilon_0\varepsilon_r\mu V^2/d^3$, where J is the current, ε_0 is the permittivity of free space, ε_r is the relative permittivity of the material, μ is the (electron) mobility, V is the applied voltage, and d is the thickness of the fullerene-derivative layer. The estimated thicknesses of thienyl fullerene and anisyl fullerene were 75 nm and 50 nm, respectively.

Fabrication of Bulk-Heterojunction OPV Devices

P3HT was purchased from Aldrich and PCBM was purchased from Frontier Carbon Corporation. The bulk-heterojunction cells were fabricated on patterned ITO-coated glass substrates. The substrate was ultrasonically cleaned by using a surfactant, rinsed in deionized water, and finalized by treatment with UV/ozone. A thin layer of PEDOT:PSS (Baytron AI 4083 from H. C. Starck) was spin-coated onto the ITO glass at a speed of 3000 rpm for 30 s in a glove box that was filled with nitrogen. Blended solutions of P3HT:fullerenes (thiophene-unit/fullerene, 1.1:0.9 molar ratio) in 1,2-dichlorobenzene (2.0 wt %) were prepared and spin-coated onto the PEDOT:PSS layer. Then, the Ca/Al electrode was evaporated onto the film through a shadow mask, thereby giving an active area of 4.00 mm^2. The photovoltaic cells were encapsulated with backing glass by using UV-curable resin under a nitrogen atmosphere.

Fabrication of OPV Devices with a p–n Heterojunction

1,4:8,11:15,18:22,25-Tetraethano-29 H,31 H-tetrabenzo[b,g,L,q]porphyrin (CP) was prepared according to literature procedures.[17] PCBM was purchased from Frontier Carbon Corporation and used as received. PEDOT:PSS (Baytron PH and AI4083) was purchased from H. C. Starck. Organic photovoltaic cells that had a *p–n* structure were fabricated according to the following typical procedure: The layer of ITO on the glass substrate was 145 nm thick with a sheet resistance of 8 ohms/square; the surface roughness (R^a) was 0.7 nm and R_{max} was 8.1 nm. A stripe pattern with a 2 mm-wide layer of ITO was etched by using a conventional photolithographic technique. Prior to the formation of the buffer layer, the patterned ITO glass was ultrasonically cleaned by using a surfactant, rinsed with water, and then finally treated with UV/ozone. A conducting poly(3,4-ethylenedioxylenethiophene)–polystyrene-sulfonic-acid (PEDOT:PSS, Baytron PH or AI4083) layer was formed on the ITO substrate by spin-coating an aqueous dispersion to obtain a smooth 30 nm-thick film. The PEDOT:PSS-coated substrate was dried in air for 10 min at 120 °C, then dried in a nitrogen glove box for 3 min at 180 °C prior to use. A precursor solution that contained 0.5 wt.% of CP in a $CHCl_3$/chlorobenzene mixture (1:2) was spin-coated (1500 rpm) onto the PEDOT:PSS layer. Thermal conversion was carried out at 180 °C for 20 min to obtain a layer of BP. After this, the fullerene derivative (0.8 wt.%) was spin-coated (3000 rpm) from a solution of CS_2/chlorobenzene (1:1, v/v) to obtain the *n* layer. After drying this film for 10 min at 120 °C, the device substrate was transferred from the glove box into the vacuum chamber without exposure to air. The evaporation of a NBphen-buffer layer was carried out at a pressure of about 2×10^{-4} Pa. The deposition rate was typically 0.1 nm s^{-1}. After the deposition of the NBphen layer (6–8 nm), the top electrode (Al, 80 nm) was deposited with a metal shadow mask, which defined a 2 mm stripe pattern that was perpendicular to the ITO stripe. Finally, the fabricated organic photovoltaic cell was encapsulated with backing glass by using a UV-curable resin under a nitrogen atmosphere.

Fabrication of OPV Devices with a p–i–n Junction

Organic photovoltaic cells that had a *p–i–n* structure were fabricated in the same manner as those with a *p–n* heterojunction (see above), except for the following point: An *i* layer was deposited on top of the BP layer (*p* layer) by spin-coating (1500 rpm) a mixture of CP and a fullerene derivative (CP, 0.3 wt.%; fullerene, 0.7 wt.%) in a $CHCl_3$/chlorobenzene/CS2 mixture (1:1:1). The *i* layer was heated at 180 °C for 20 min. After this, the *n* layer was spin-coated in the same manner.

Acknowledgements

This work was generously supported by the Funding Program for Next-Generation World-Leading Researchers (Y.M.), MEXT, Japan (KAKENHI to E.N., 22000008), and the Strategic Promotion of Innovative Research and Development from the Japan Science and Technology Agency (JST).

---

[1] a) J. C. Hummelen, B. W. Knight, F. LePeq, F. Wudl, J. Yao, C. L. Wilkins, *J. Org. Chem.* **1995**, *60*, 532; b) F. B. Kooistra, J. Knol, F. Kastenberg, L. M. Popescu, W. J. H. Verhees, J. M. Kroon, J. C. Hummelen, *Org. Lett.* **2007**, *9*, 551.

[2] G. Yu, J. Gao, J. C. Hummelen, F. Wudl, A. J. Heeger, *Science* **1995**, *270*, 1789.

[3] a) Y. Matsuo, A. Iwashita, Y. Abe, C. Z. Li, K. Matsuo, M. Hashiguchi, E. Nakamura, *J. Am. Chem. Soc.* **2008**, *130*, 15429; b) Y. Matsuo, Y. Sato, T. Niinomi, I. Soga, H. Tanaka, E. Nakamura, *J. Am. Chem. Soc.* **2009**, *131*, 16048; c) H. Tsuji, K. Sato, Y. Sato, E. Nakamura, *Chem. Asian J.* **2010**, *5*, 1294; d) H. Tsuji, Y. Yokoi, Y. Sato, H. Tanaka, E. Nakamura, *Chem. Asian J.* **2011**, *6*, 2005; e) H. Tanaka, Y. Abe, Y. Matsuo, J. Kawai, I. Soga, Y. Sato, E. Nakamura, *Adv. Mater.* **2012**, *24*, 3521.

[4] a) Y. Matsuo, Y. Zhang, I. Soga, Y. Sato, E. Nakamura, *Tetrahedron Lett.* **2011**, *52*, 2240; b) A. Varotto, N. D. Treat, J. Jo, C. G. Shuttle, N. A. Batara, F. G. Brunetti, J. H. Seo, M. L. Chabinyc, C. J. Hawker, A. J. Heeger, F. Wudl, *Angew. Chem.* **2011**, *123*, 5272; *Angew. Chem. Int. Ed.* **2011**, *50*, 5166.

[5] M. Lenes, G.-J. A. H. Wetzelaer, F. B. Kooistra, S. C. Veenstra, J. C. Hummelen, P. W. M. Blom, *Adv. Mater.* **2008**, *20*, 2116.

[6] a) D. W Laird, H. Richter, V. Vejins, L. Scott, T. A Lada, II, WO/2008/018931; US Patent Application 20090176994; b) Y. He, H.-Y. Chen, J. Hou, Y. Li, *J. Am. Chem. Soc.* **2010**, *132*, 1377; c) Y. He, G. Zhao, B. Peng, Y. Li, *Adv. Funct. Mater.* **2010**, *20*, 3383; d) G. Zhao, Y. He, Y. Li, *Adv. Mater.* **2010**, *22*, 4355; e) Y.-J. Cheng, C.-H. Hsieh, Y. He, C.-S. Hsu, Y. Li, *J. Am. Chem. Soc.* **2010**, *132*, 17381.

[7] a) Y. Zhang, Y. Matsuo, C.-Z. Li, H. Tanaka, E. Nakamura, *J. Am. Chem. Soc.* **2011**, *133*, 8086; b) C.-Z. Li, S.-C. Chien, H.-L. Yip, C.-C. Chueh, F.-C. Chen, Y. Matsuo, E. Nakamura, A. K.-Y. Jen, *Chem. Commun.* **2011**, *47*, 10082; c) C.-Z. Li, Y. Matsuo, E. Nakamura, *Tetrahedron* **2011**, *67*, 9944.

[8] Y. Matsuo, A. Ozu, N. Obata, N. Fukuda, H. Tanaka, E. Nakamura, *Chem. Commun.* **2012**, *48*, 3878.

[9] J. Guo, H. Ohkita, H. Benten, S. Ito, *J. Am. Chem. Soc.* **2010**, *132*, 6154.

[10] a) B. Barszcz, B. Laskowska, A. Graja, E. Y. Park, T.-D. Kim, K.-S. Lee, *Chem. Phys. Lett.* **2009**, *479*, 224; b) K. Yoshimura, K. Matsumoto, Y. Uetani, S. Sakumichi, S. Hayase, K. Kawatsura, T. Itoh, *Tetrahedron* **2012**, *68*, 3605.

[11] Y. Zhang, Y. Matsuo, E. Nakamura, *Org. Lett.* **2011**, *13*, 6058.

[12] A. Iwashita, Y. Matsuo, E. Nakamura, *Angew. Chem.* **2007**, *119*, 3583; *Angew. Chem. Int. Ed.* **2007**, *46*, 3513.

[13] a) M. Nambo, R. Noyori, K. Itami, *J. Am. Chem. Soc.* **2007**, *129*, 8080; b) S. Mori, M. Nambo, L.-C. Chi, J. Bouffard, K. Itami, *Org. Lett.* **2008**, *10*, 4609.

[14] a) P. D. W. Boyd, M. C. Hodgson, C. E. F. Rickard, A. G. Oliver, L. Chaker, P.-J. Brothers, R. D. Bolskar, F. S. Tham, C. A. Reed, *J. Am. Chem. Soc.* **1999**, *121*, 10487; b) D. V. Konarev, R. N. Lyubovskaya, N. V. Drichko, E. I. Yudanova, Y. M. Shul'ga, A. L. Litvinov, V. N. Semkin, V. P. Tarasov, *J. Mater. Chem.* **2000**, *10*, 803.

[15] C.-Z. Li, Y. Matsuo, T. Niinomi, Y. Sato, E. Nakamura, *Chem. Commun.* **2010**, *46*, 8582.

[16] a) A. Saeki, S. Seki, T. Sunagawa, K. Ushida, S. Tagawa, *Philos. Mag.* **2006**, *86*, 1261; b) A. Saeki, S. Seki, Y. Koizumi, S. Tagawa, *J. Photochem. Photobiol. A* **2007**, *186*, 158; c) A. Saeki, M. Tsuji, S. Seki, *Adv. Energy Mater.* **2011**, *1*, 661; d) A. Saeki, Y. Yamamoto, Y. Koizumi, T. Fukushima, T. Aida, S. Seki, *J. Phys. Chem. Lett.* **2011**, *2*, 2549.

[17] a) S. Ito, T. Murashima, H. Uno, N. Ono, *Chem. Commun.* **1998**, 1661; b) S. Aramaki, Y. Sakai, N. Ono, *Appl. Phys. Lett.* **2004**, *84*, 2085.

Received: August 8, 2012